JOURNAL OF Materials CHEMISTRY

Crystal growth of a stable nonlinear optical organic material: 2-amino-5-nitropyridinium monohydrogen L-tartrate

Julien Zaccaro,[a] Frédéric Lorut[b] and Alain Ibanez[a]*

[a]*Laboratoire de Cristallographie, C.N.R.S., associé à l'Université J. Fourier et à l'Institut National Polytechnique de Grenoble, BP 166, F-38042, Grenoble Cedex 09, France*
[b]*European Synchrotron Radiation Facility, BP 220, F-38043, Grenoble Cedex, France*

Received 24th December 1998, Accepted 18th February 1999

We report on the optimization of synthesis, solubility and crystal growth from solution of 2-amino-5-nitropyridinium L-tartrate (labelled 2A5NPLT). This newly engineered guest–host hydrogen-bonding salt exhibits a quasi-perfect polar alignment of the nonlinear chromophores in the crystalline lattice which is promising for optimized Pockels electrooptic properties. In addition, the dense and 3D-intermolecular framework built up by short hydrogen bonds leads to improved thermal, mechanical and chemical stability compared with that of organic molecular crystals. The solvent selection allowed the elaboration of bulky crystal by the temperature lowering method. Synchrotron X-ray diffraction topography experiments carried out on uncut crystals revealed a high crystalline perfection.

Introduction

In the last two decades, extensive research has shown that organic crystals can exhibit nonlinear optical (NLO) efficiencies which are two orders of magnitude higher than those of inorganic materials.[1,2] This is due to highly polarizable molecules involving conjugated systems of π electrons such as polyenes or aromatic compounds. These organic phases possess other advantages such as unlimited molecular engineering and often high laser damage thresholds. In addition, large single crystals can be grown from solution close to room temperature.[3,4] Nevertheless, due to their poor chemical stability and low thermal and mechanical resistance, the use of organic molecular crystals is currently limited in their NLO industrial applications. An added drawback is that the polar nature of these phases with one- or two-dimensional structures leads to important problems in crystal growth and processing of optical devices.

In order to overcome these difficulties, a strategy has recently been developed which aims to build very cohesive acentric crystalline structures based on host–guest chemistry.[5] The anchorage of highly polarizable chromophores onto various inorganic or organic anionic matrices leads to short and multiple hydrogen-bonded networks. Several polarizable molecules were selected in this crystal engineering and particularly 2-amino-5-nitropyridine (2A5NP). A great number of salts having a 3D acentric structure based on herringbone motifs were obtained with this push–pull molecule such as the dihydrogen phosphate,[6] dihydrogen arsenate,[7] chloride, bromide,[8] chloroacetate[9] and acetophosphonate of 2-amino-5-nitropyridinium.[10] These salts possess enhanced stability (chemical, thermal, mechanical) compared to the corresponding molecular organic crystals. Moreover, they exhibit a wider transparency range and bulky crystal morphology.[11,12] The first qualitative evaluations of the nonlinear response (powder tests of second harmonic generation[13]) showed high efficiencies for all these materials. These results are confirmed by the first nonlinear characterizations carried out on single crystals.[14–16] Furthermore, optical parametric oscillation has just been demonstrated with the 2-amino-5-nitropyridinium dihydrogen phosphate (2A5NPDP) compound.[17]

From this crystal engineering, another type of salt structure was evidenced. Indeed, in the crystal structure of 2-amino-5-nitropyridinium L-tartrate (2A5NPLT), space group $P2_1$ with $a=8.248$ Å, $b=9.199$ Å, $c=7.611$ Å and $\beta=96°.5$,[18] the $2A5NP^+$ cations are nearly aligned along the *b*-axis. In addition, their H-bonding anchoring onto the polyanionic helical tartrate chains is very dense leading to a 3D framework (Fig. 1). A first NLO characterization showed a large susceptibility coefficient $d_{33}=41$ pm V^{-1} at $\lambda=1.06$ μm.[19] Moreover, the alignment of the dipole moments in the 2A5NPLT crystalline lattice is promising for optimized Pockels electrooptic properties. Thus, in order to specify these NLO potentialities, we have undertaken the elaboration of high quality 2A5NPLT crystals. Our first results obtained on the synthesis optimization, solubility and crystal growth from solution are displayed here. Then, a morphological study of 2A5NPLT is introduced. Finally, we have determined their transparency bandwidth, the thermal and mechanical stability while the crystalline quality was defined using synchrotron X-ray topography.

Synthesis and solubility

The 2A5NP molecule is a weak Brønsted base which can be protonated in a strong acidic medium (pH <2). This induces the dissolution of this molecule in aqueous acidic solutions by formation of the 2-amino-5-nitropyridinium cation ($2A5NP^+$) and leads to the synthesis of hydrogen-bonded salts with the conjugated bases of strong or medium acids ($pK_a<3.3$). In the case of tartaric acid, the 2A5NPLT phase can be directly obtained by reaction (1).

$$C_5H_5N_3O_2 + \text{L-}C_4H_6O_6 \longrightarrow C_5H_6N_3O_2^+ + \text{L-}C_4H_5O_6^- \longrightarrow C_5H_6N_3O_2^+ \cdot C_4H_5O_6^- \quad (1)$$

(2A5NP) (2A5NPLT)

Nevertheless, tartaric acid is a too weak Brønsted acid that does not completely dissolve the 2A5NP powder in aqueous solutions due to partial 2A5NP protonation. This explains the low synthesis yields, around 50%. We have optimized the 2A5NPLT synthesis by using acetic acid as an intermediate solvent. Indeed, this acid ($pK_a=4.76$) does not react with 2A5NP but makes it possible, at high concentrations (13–16 M), to reach low pH values (pH <1) and to completely dissolve the amount of 2A5NP in reaction (1). Thus, the 2A5NPLT salt is obtained by first dissolving the 2A5NP in an acetic acid solution (16 M) at 60 °C. Then, a saturated tartaric aqueous solution (4 M) is added. The molar ratios are 1 : 1 : 5 : 5 for 2A5NP, $C_4H_6O_6$, CH_3COOH and H_2O respectively. The

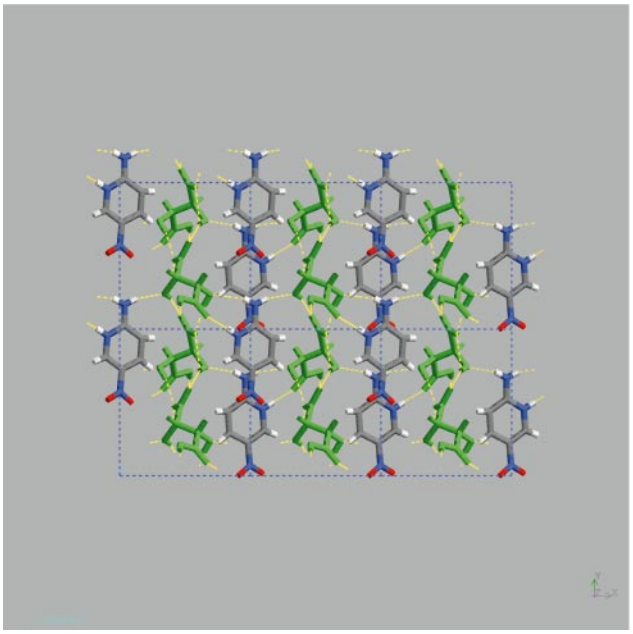

Fig. 1 Projection of the polar structure of 2A5NPLT in the **ab** plane showing a quasi-perfect alignment of the 2-amino-5-nitropyridinium cations.

salt crystallizes at room temperature as a white microcrystalline powder on addition of acetone. Thus, the synthesis yield is close to 100%. In order to increase the crystal quality, we take particular care in ensuring the purity of the starting materials. The commercial 2A5NP is first purified by double sublimation and then dissolved in high purity acidic solutions. Finally, the salts are purified again from CH_3COOH solutions, by recrystallization in acetone.

Due to the thermal decomposition of 2A5NPLT (see Stability section), we have undertaken the crystal growth of this phase from acidic solutions. We first selected as solvent the acid corresponding to the salt. We determined the solubility curves between 20 and 60 °C for various molar concentrations of tartaric acid (2–4 M) which satisfy the pH conditions (pH <2). Unfortunately, the magnitude of the 2A5NPLT solubility (S) and its variation with temperature (solubility–temperature gradient $\Delta S/\Delta T$) in these concentrated aqueous solutions are always very low (Fig. 2).

On the other hand, we have seen for other salts of this family that the solubility curve is directly related to the pH of the growth solution; the lower the pH value, the higher are the solubility and the solubility–temperature gradient.[11,12] As previously mentioned, acetic acid aqueous solutions (13–16 M) allow low pH values to be achieved without combining with the 2A5NP molecule. Thus, we registered in these acetic solutions higher 2A5NPLT solubilities and solubility–temperature gradients than in tartaric solvent (Fig. 2). Despite these increases, S and $\Delta S/\Delta T$ remain rather low for the use of the typical temperature lowering (TL) method. Thus, in order to adjust the 2A5NPLT solubility, another solvent was used: formic acid ($pK_a = 3.75$) which does not react with 2A5NP. Indeed, as for acetic acid, low pH solutions can be achieved at high concentrations (HCOOH 10–20 M). In these formic acid solutions we have obtained an important increase of S and $\Delta S/\Delta T$ compared to tartaric and acetic solvents (Fig. 2). These significant evolutions allow a great flexibility for selecting the growth technique and optimizing crystal growth conditions.

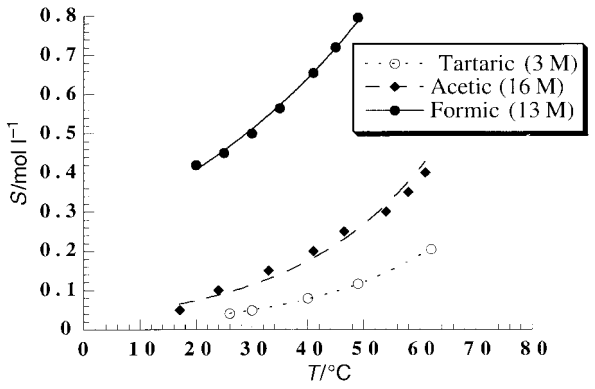

Fig. 2 Solubility curves of the 2A5NPLT salt in tartaric (3 M), acetic (16 M) and formic acid (13 M) aqueous solutions.

Crystal growth and morphology

The first growths of 2A5NPLT crystals were carried out in tartaric acid solutions (3 M). The low $\Delta S/\Delta T$ value for this solvent prompted us to select thermal gradient methods. A horizontal temperature-gradient technique (HTG) was used to obtain high-quality seeds by spontaneous nucleation. Nevertheless, this growth reactor, described elsewhere,[12] does not allow the growth of large single crystals. In addition, the resulting crystals exhibit a lot of growth bands evidenced by X-ray diffraction topography[12] because the seeds and the growth solution are not stirred. Thus, in order to obtain large crystals of high quality we then used a vertical temperature-gradient method (VTG).[20] The nutrient comprises millimetric 2A5NPLT crystals placed in the upper zone of a container of controlled porosity. The thermal configuration, with a higher temperature in the upper zone ($\Delta T \approx 3$–4 °C), reduces the natural convection. The seeds, previously grown by the HTG method, are stacked to silica suspensions in the lower zone and are rotated at a rate of 20 rpm with inversion of the rotation direction every 40 s. Thus, after 3–4 months of growth, large and optically clear crystals are obtained [Fig. 3(a)]. Unfortunately, these 2A5NPLT crystals have weak growth rates, around 0.1–0.2 mm day^{-1}, and a plate morphology. This crystal morphology was determined from X-ray diffraction (Laüe diagrams) and interfacial angle measurements using a two-circle optical goniometer (Nedinsco) [Fig. 4(a)]. The crystal morphology has been drawn with the program SHAPE,[21,22] using the experimental growth rates as the face-crystal center in the Wulff plot. The 2A5NPLT plate habit is mainly due to a very low growth rate of the {101} form. In contrast to other salts of this family,[11,12] the 2A5NPLT phase grows in a number of well faceted forms of low Miller's indexes [Fig. 4(a)].

Then, in order to obtain bulky crystals, we used another growth solvent. As we also obtain platelet crystals with acetic acid, we selected formic acid solutions which lead to bulky crystals. Moreover, the higher solubility and solubility–temperature gradient values registered for this solvent allow us to carry out the 2A5NPLT crystal growth by the typical temperature lowering (TL) method. For a good control of crystal growth, the temperature lowering rates have to be less than 0.2 °C per day at low relative supersaturations around 0.01. This requires a high temperature precision (± 0.002 °C) to avoid undesirable supersaturation changes leading to secondary nucleation, macro steps and multiple solvent inclusions on the growing crystal faces. These growth problems are favored in this case by a narrow metastable zone. The growth solution (around 200 cm^3) is seeded with 2A5NPLT crystal about 1 mm^3 in size, obtained by spontaneous nucleation in the same TL crystallizer previously described.[11] The growing crystals are rotated (20–30 rpm) and are reversed every 45 s. The temperature is slowly decreased in the range 45–35 °C. This second set of growth experiments allowed us to obtain in 2–3 months bulky and optically clear crystals [Fig. 3(b)]. This bulky morphology is essentially achieved through a

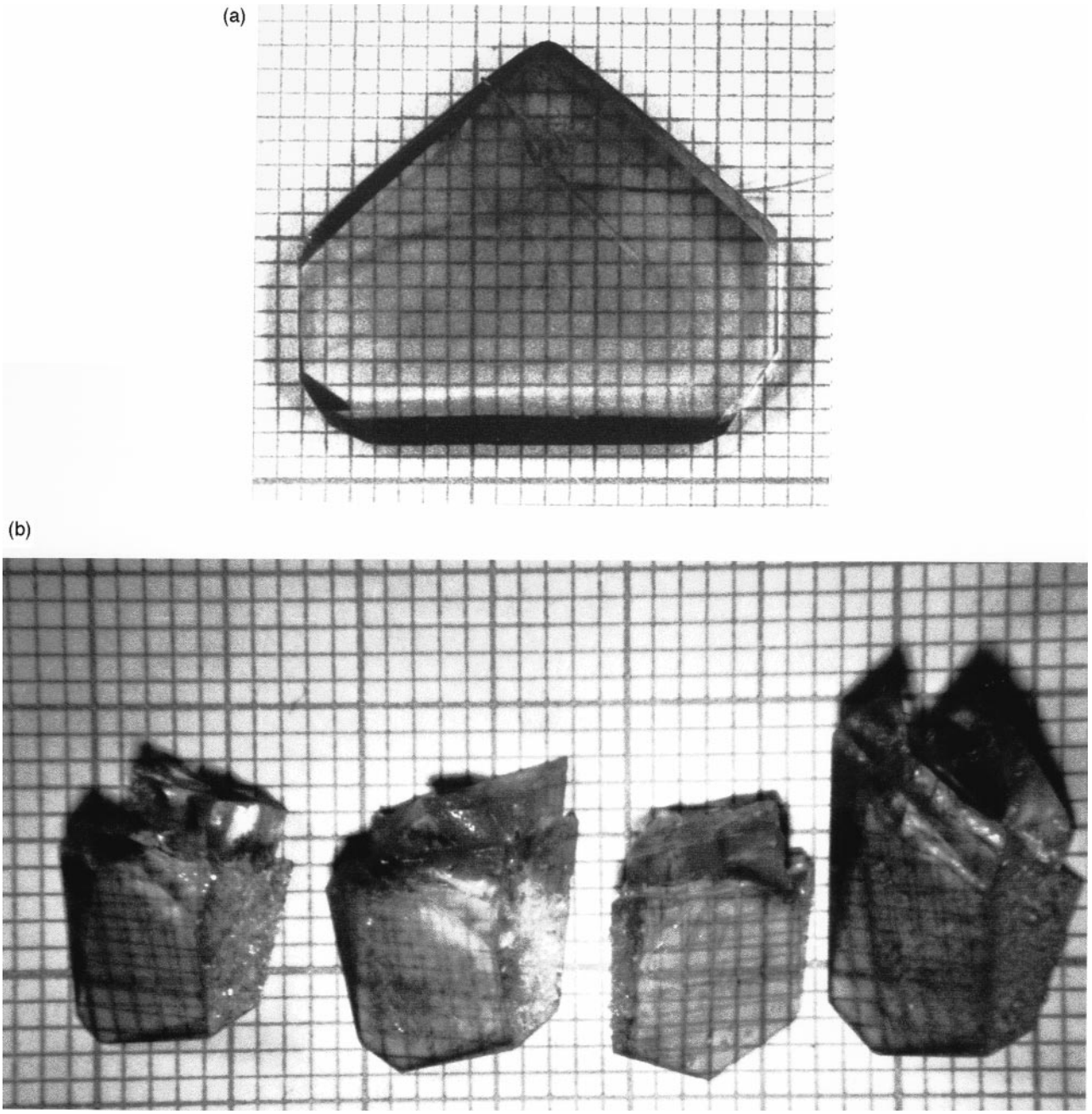

Fig. 3 2A5NPLT crystals grown (a) by the HTG method in tartaric acid solutions (3 M), (b) by the LT technique in formic acid (13 M) aqueous solutions.

significant increase of the {101} growth rate [Fig. 4(b)]. Unfortunately, the average growth rates remain very weak (less than 0.2 mm day^{-1}). This is certainly due to the adsorption of polar solvent molecules on the crystal faces of this highly polar material.

Crystal characterizations

Stability

A differential scanning calorimetry study associated with thermogravimetry experiments showed that the 2A5NPLT phase is decomposed at temperatures over 195 °C following the chemical reaction:

$$C_5H_6N_3O_2^+ \cdot C_4H_5O_6^- \longrightarrow C_5H_5N_3O_2 + C_4H_6O_6 \quad (2)$$

This thermal stability is the best of all the H-bonded salts obtained with the 2A5NP chromophore.[11,12] In addition, the 2A5NPLT crystals have no mechanical cleavage plane. On the other hand, hardness measurements were carried out using a Leitz Vickers hardness tester. Indentations were made on (101), (001), (111), (1-11) and (1-1-1) growth faces with a dwelling time kept constant at 15 s and weights ranging from 15–25 g. In agreement with the 3D crystal structure, all these experiments gave the same average value of 105 ± 5 kg mm^{-2}. The 2A5NPLT hardness is the highest of the 2A5NP salt family and is rather close to that of KDP (135 kg mm^{-2}). These good mechanical properties make slicing and polishing easier for the optical device processing of 2A5NPLT crystals. Finally, this tartrate possesses the lowest moisture sensitivity of the 2A5NP salt family, the surfaces of the crystal plates being perfectly stabilized under a dry atmosphere.

Crystalline perfection

Crystal quality assessment can be performed using X-ray diffraction techniques such as X-ray diffraction topography which provides a map of defects and strains in crystals.

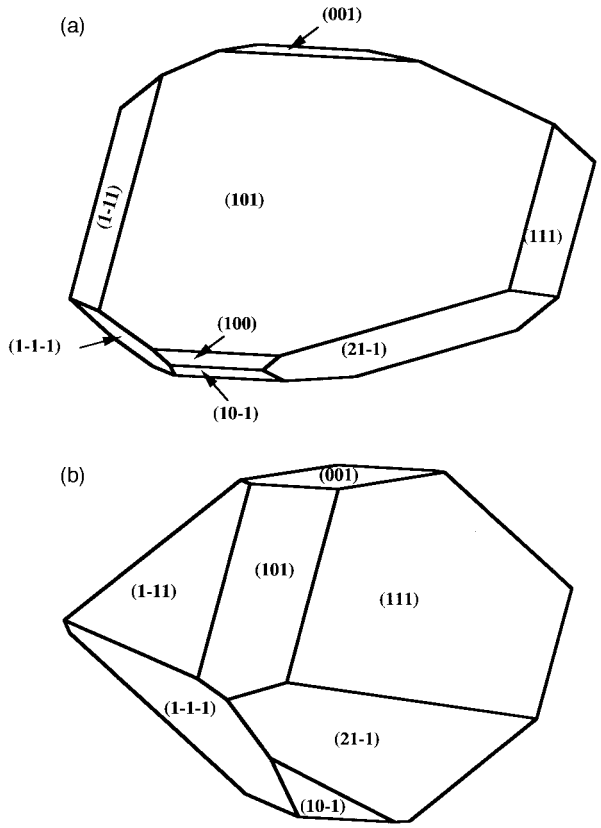

Fig. 4 Typical morphologies of 2A5NPLT crystals grown in (a) tartaric acid or (b) in formic acid aqueous solutions.

Moreover, the new possibilities associated with the third-generation synchrotron sources[23] allow the investigation of thick and absorbing materials with short exposure times (10^{-2}–10^{2} s) and with high spatial resolution for diffracted images (≈ 1 μm). Section topography consists of intersecting a narrow collimating slit (20 μm in this study) before the crystal in order to reduce the white X-ray beam extension in one direction. Thus, the image recorded onto the film located behind the sample (Laüe transmission geometry) can be considered as a projection of the virtual slice of the crystal traversed by the beam (Fig. 5). As a small part of the sample is illuminated, the defect images are more easily distinguished than in conventional transmission topography. The section topographs were recorded at the ESRF, on the ID19 beamline. We characterized non-destructively the crystalline quality of the as-grown 2A5NPLT crystals using a beam absorber (6 mm of Al) to avoid heat load on the samples. In this configuration, we do not observe any crystal damage or image contrast evolution. At these low X-ray wavelengths (0.1 Å $< \lambda <$ 1 Å) the product of the mass absorption coefficient, μ, and the crystal thickness, t, was $\mu t < 1$. These section topographs allow simultaneous characterization of the growth process and the crystalline quality at a given moment of the growth.

Fig. 6 shows section topographs of a 2A5NPLT crystal grown by the TL method in formic acid aqueous solutions (13 M). On the right hand side of Fig. 6 we have given schematic representations of the positions of the main features of the corresponding topographs. These three topographs were recorded perpendicularly to the c-axis with a sample–film distance of 20 cm (Fig. 5). Between these exposures the crystal was moved up by 3 mm along the c-axis. Since the section topographs were recorded from a crystal with fully developed morphology, the diffracted images show rather well defined crystal edges corresponding to the (1 −1 1), (1 1 1), (−1 1 −1) and (−2 −1 1) faces. The weak image contrast of all these section topographs reveals a high crystalline perfection

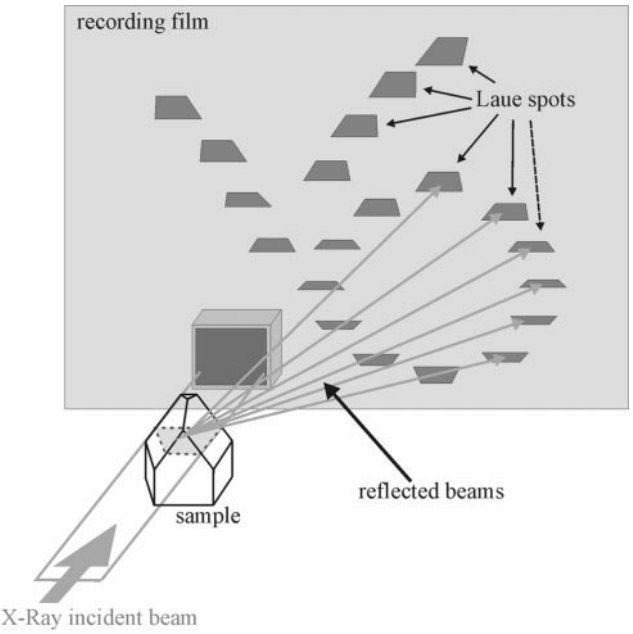

Fig. 5 Schematic representation of the experimental set up of the synchrotron section topography on the ID19 beamline (ESRF Grenoble). The 2A5NPLT crystal position is also specified (the **c** axis is vertical).

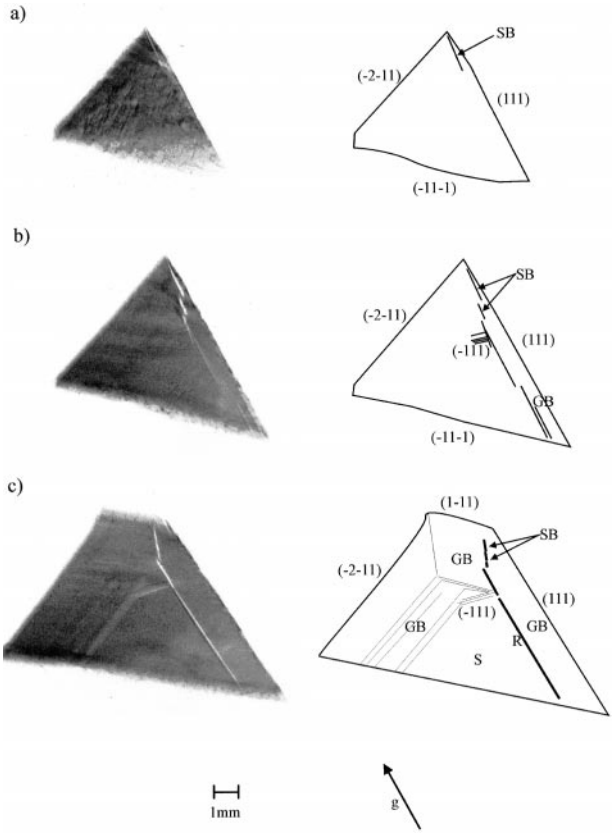

Fig. 6 Section topographs of a 2A5NPLT crystal recorded perpendicularly to the **c** axis. The main features of these topographs are represented in their corresponding outline diagrams.

of 2A5NPLT crystals without any large defect. Nevertheless, typical defects, which are likely to be associated with solution-grown crystals, namely, seed position (S), growth sector boundaries (SB) and growth bands (GB), can be observed. In Fig. 6(c) the central seed (S) can be easily detected through the growth restart interface (R) while sections 6b and 6a are those away from the seed. The interface between the seed

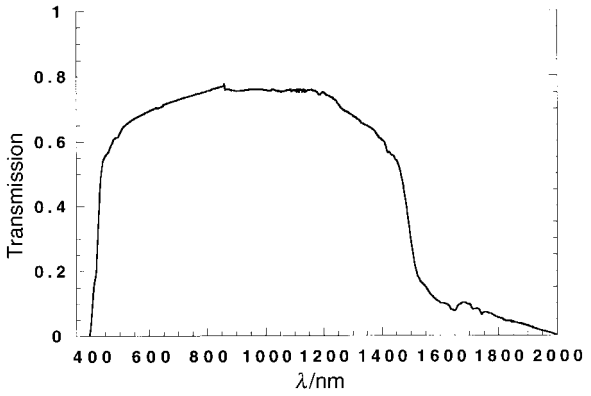

Fig. 7 Optical transmission spectrum of 2A5NPLT crystal measured perpendicularly to the (001) plate of 3 mm thickness.

and the crystal is not very strained, probably due to careful control of the initial growth onto the seed. The seed exhibits a low defect density due to the adjustment of the homogeneous nucleation conditions involved for the elaboration of millimetric seeds by the HTG or LT methods.

On the other hand, the position and the nature of the growth sector boundaries display a clear insight into the growth history of the crystal. Thus, we can see in Fig. 6(c) the disappearance of the (–111) face due to its rapid growth rate which is associated with growth bands (GB). These growth bands must arise from the incorporation of either solvent or other impurities into the growing crystal face. We find also GB contrasts in the (1 −1 1), (1 1 1) and (−2 −1 1) sectors which reveal low varying growth conditions. This explains the irregular growth sector boundary (SB, Fig. 6(b)) due to fluctuations in the relative growth rates between the (1 −1 1) and (1 1 1) faces during the growth (Fig. 6(c), (b) and (a)). The other growth sector boundary, between (1 −1 1) and (−2 −1 1), is almost perfectly straight and weakly visible, indicating that the relative growth rates of the two sectors are uniform. The lack of a (−1 1 −1) sector reveals a very low growth rate of this face in constrast to the opposite one (1 −1 1) in agreement with the highly polar structure of this organic salt. During the whole growth process, and starting from a high quality seed, we observe a high crystalline perfection in the different growth sectors.

Optical transmission

The sample was a 3 mm-thick (001) plate of a 2A5NPLT crystal grown by the TL method in formic acid solution. The absorption spectrum (Fig. 7), recorded with a Perkin-Elmer λ9 spectrometer, shows a lower cut-off (defined at 50% transmittance) at 410–420 nm. As previously discussed for other salts obtained with the 2A5NP molecule,[14,24] this cut-off is due to an electronic transition of the 2A5NP chromophore. On the other hand, the absorption band in the near IR region (1650 nm) can be attributed to the overtone of C–H vibration followed by a large absorption band starting near 2000 nm which is typically assigned to aromatic rings (2A5NP).

Conclusions

The 2A5NPLT salt exhibits a quasi-perfect polar alignment of nonlinear chromophores in a dense and 3D-intermolecular framework built up by short hydrogen bonds. This crystal structure leads to good thermal, mechanical and chemical stability. These properties associated with a high optical efficiency and a transparency bandwidth from 410 to 1500 nm give to 2A5NPLT interesting potentiality for electooptic devices. We have optimized the synthesis of this salt and have selected the growth solution (formic acid 13 M) which leads to bulky crystals. The choice of the growth method was based on the temperature-dependent solubility. The best growth results were obtained in aqueous formic acid solution (13 M) using the TL method. Synchrotron X-ray diffraction topography experiments carried out on large uncut crystals revealed a high crystalline perfection. The 2A5NPLT crystals are easily sliced and polished without any cleavage plane and are stable and suitable for optical characterizations. The unique remaining drawback is the weak growth rate (around 0.1–0.2 mm day^{-1}) obtained in all these 2A5NPLT growths in solution. For this reason we are working now on the adjustment of rapid growth conditions.

Acknowledgements

The authors thank R. Masse (Lab. Cristallographie, CNRS-Grenoble) and J. Baruchel (ESRF-Grenoble) for the critical reading of this manuscript, and P. L. Baldeck (Lab. Spectrométrie Physique, UJF) for optical transmission measurements.

References

1 J. Zyss, J. F. Nicoud and M. Coquillay, *J. Chem. Phys.*, 1984, **81**, 4160.
2 I. Ledoux, J. Badan, J. Zyss, A. Migus, D. Hulin, J. Etchepare, G. Grillon and A. Antonetti, *J. Opt. Soc. Am. B*, 1987, **4**, 987.
3 R. Hierle, J. Badan and J. Zyss, *J. Cryst. Growth*, 1984, **69**, 545.
4 B. Y. Shekkunov, E. A. Shepherd, J. N. Sherwood and G. S. Simpson, *J. Phys. Chem.*, 1995, **99**, 7130.
5 R. Masse, M. Bagieu-Beucher, J. Pécaut, J. P. Lévy and J. Zyss, *Nonlinear Optics*, 1993, **5**, 413.
6 R. Masse and J. Zyss, *Mol. Eng.*, 1991, **1**, 141.
7 J. Pécaut, Y. Le Fur and R. Masse, *Acta Crystallogr., Sect. B*, 1993, **49**, 535.
8 J. Pécaut, J. P. Lévy and R. Masse, *J. Mater. Chem.*, 1993, **3**, 999.
9 Y. Le Fur, M. Bagieu-Beucher, R.Masse, J. F. Nicoud and J. P. Lévy, *Chem. Mater.*, 1995, **8**, 68.
10 J. Pécaut and R. Masse, *J. Mater. Chem.*, 1994, **4**, 1851.
11 A. Ibanez, J. P. Levy, C. Mouget and E. Prieur, *J. Solid State Chem.*, 1997, **129**, 22.
12 J. Zaccaro, B. Capelle and A. Ibanez, *J. Cryst. Growth*, 1997, **180**, 229.
13 S. K. Kurtz and T. T. Perry, *J. Appl. Phys.*, 1968, **39**, 3798.
14 Z. Kotler, R. Hierle, D. Josse, J. Zyss and R. Masse, *J. Opt. Soc. Am. B*, 1992, **9**, 534.
15 N. Horiuchi, F. Lefaucheux, M. C. Robert, D. Josse and J. Zyss, *J. Cryst. Growth*, 1995, **147**, 361.
16 J. P. Feve, B. Boulanger, I. Rousseau, G. Marnier, J. Zaccaro and A. Ibanez, *IEEE J. Quantum Electron.*, 1999, **35**, 403.
17 S. Khodja, D. Josse and J. Zyss, *J. Opt. Soc. Am. B*, 1998, **15**, 751.
18 J. Zyss, R. Masse, M. Bagieu-Beucher and J. P. Lévy, *Adv. Mater.*, 1993, **5**, 120.
19 O. Watanabe, T. Noritake, Y. Hirose, A. Okada and T. Kurauchi, *J. Mater. Chem.*, 1993, **3**, 1053.
20 J. Zaccaro, M. Bagieu-Beucher, J. Espeso and A. Ibanez, *J. Cryst. Growth*, 1998, **186**, 224.
21 E. Dowty, SHAPE, 521 Hidden Valley Road, Kingsport, TN 37663; Copyright 1989.
22 E. Dowty, *Am. Mineral.*, 1980, **65**, 465.
23 R. Barret, J. Baruchel, J. Härtwig and F. Zontone, *J. Phys. D. Appl. Phys.*, 1995, **28**, A250.
24 J. Zaccaro, D. Block, M. Chamel and A. Ibanez, submitted to *J. Opt. Soc. Am. B.*

Paper 8/10005E